

## Supporting Information

### **Ultrathin and flexible PDA modified MXene/bacterial cellulose composite film with densely lamellar structure for enhanced electromagnetic interference shielding performance**

Cuilian Wen <sup>a,\*</sup>, Hao Liu <sup>a,\*</sup>, Lijin Luo <sup>b</sup>, Zhou Cui <sup>a</sup>, Xiong Li <sup>a</sup>, Junhao Jin <sup>a</sup>, Siqing Yan <sup>a</sup>,

Peng Lin <sup>a</sup>, Baisheng Sa <sup>a,\*</sup>

<sup>a</sup>*Multiscale Computational Materials Facility & Materials Genome Institute, School of Materials Science and Engineering, Fuzhou University, Fuzhou 350100, China.*

<sup>b</sup>*Fujian Institute of Microbiology, Fuzhou 350007, China*

#### **Corresponding authors:**

*E-mail addresses:* clwen@fzu.edu.cn (C. Wen), liuhao2092023@163.com (H. Liu),

bssa@fzu.edu.cn (B. Sa)

Compared with previous reported functional materials (Table S1), the PM/BC composite film synthesized in this work has superior mechanical properties, showing great potential in practical applications of electronic products.

**Table S1.** The comparison of mechanical properties of PM50/BC composite film and other reported composites.

| Sample | Materials  | Tensile strength |            | Refs.     |
|--------|--|------------------|------------|-----------|
|        |  | (MPa)            | Strain (%) |           |
| 1      | Ti <sub>3</sub> C <sub>2</sub> T <sub>x</sub> /ANF     | 197.1            | 9.80       | 1         |
| 2      | Nacre  | 135.0            | 0.85       | 2         |
| 3      | RGP/CNF  | 156.5            | 3.90       | 3         |
| 4      | Ti <sub>3</sub> C <sub>2</sub> T <sub>x</sub> /CNF     | 112.5            | 4.30       | 4         |
| 5      | Ti <sub>3</sub> C <sub>2</sub> T <sub>x</sub> /PVA     | 91               | 3.70       | 5         |
| 6      | RGP/MG/PVA   | 62.4             | 4.50       | 6         |
| 7      | PPy@ Ti <sub>3</sub> C <sub>2</sub> T <sub>x</sub> /BC | 46.0             | 4.40       | 7         |
| 8      | LG   | 54.0             | 3.20       | 8         |
| 9      | GP/TiO <sub>2</sub> -epoxy                             | 75.0             | 1.20       | 9         |
| 10     | Cellulose/GP/PPy                                       | 90.8             | 10.00      | 10        |
| 11     | Ti <sub>3</sub> C <sub>2</sub> T <sub>x</sub> film     | 22.0             | 1.00       | 5         |
| 12     | PM50/BC  | 178.1            | 6.90       | This work |

In MXene/BC composite film, there is a noticeable void structure between the randomly arranged MXene nanosheets and BC substrate. This void structure significantly affects the compactness of the internal film structure. Additionally, the surface of MXene/BC composite film appears highly uneven, with clear delamination phenomena observed, which can result in the separation of MXene nanosheets and detachment from BC substrate during practical applications (Fig. S1).

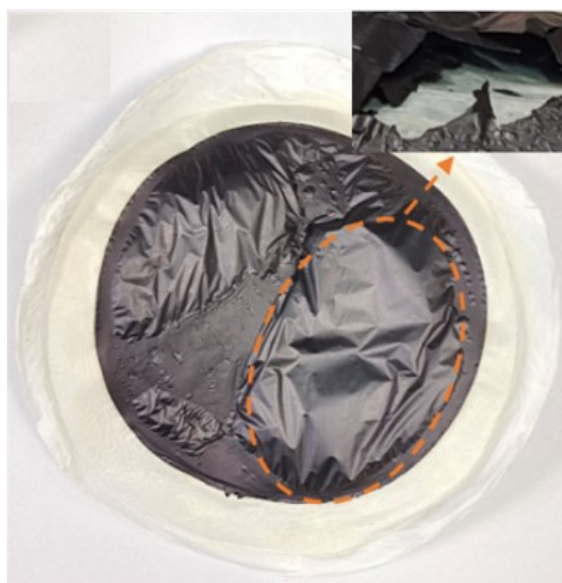


**Fig. S1.** The digital photograph of the MXene/BC composite film.

The FTIR result in Fig. S2 reveals that the surface of MXene contains -OH, -F, and -O functional groups, which are mainly dominated by hydroxyl groups. It is noted that the shifts in the -OH functional groups on the PDA/MXene surface, confirm a distinct interaction between PDA and MXene nanosheets. This plays a crucial role in determining the surface chemistry and reactivity of MXene, facilitating interactions with PDA and BC, leading to enhanced bonding and composite formation.

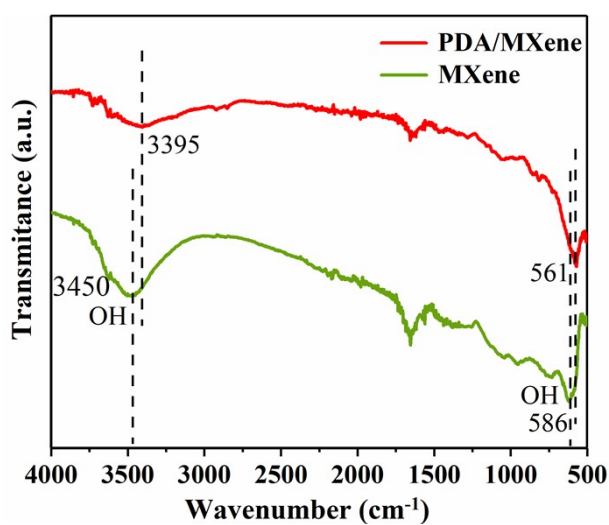


**Fig. S2.** The FTIR spectra of the  $Ti_3C_2T_x$  MXene and PDA/MXene.

To elucidate the fracture mechanism of the PM/BC composite film, we scrutinized the fracture surface of the PM50/BC composite. Fig. S3a shows a tightly packed multilayer structure characterized by 'zigzag' cracks in the BC substrate. These cracks are a testament to the robust hydrogen bonding and the efficient absorption of external forces by the BC nanofibers. Conversely, the PMXene layer displays 'plane' cracks, indicative of a brittle fracture behavior, as depicted in Fig. S3b.

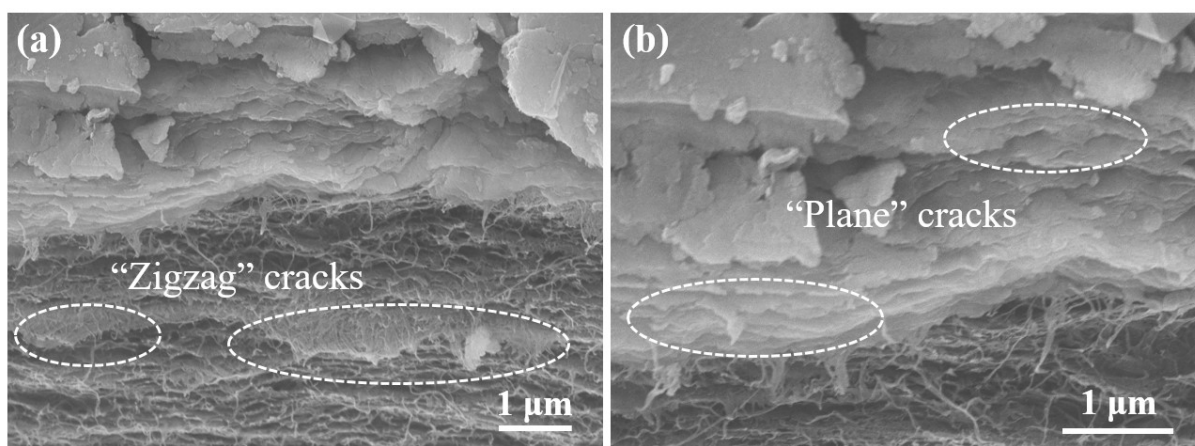


**Fig. S3.** (a) SEM image of the fracture section of PM50/BC composite film and (b) the corresponding enlarged morphology.

## References

1. F. Xie, F. Jia, L. Zhuo, Z. Lu, L. Si, J. Huang, M. Zhang and Q. Ma, *Nanoscale*, 2019, **11**, 23382-23391.
2. A. P. Jackson, J. F. V. Vincent and R. M. Turner, *J. Mater. Sci.*, 1990, **25**, 3173-3178.
3. W. Yang, Z. Zhao, K. Wu, R. Huang, T. Liu, H. Jiang, F. Chen and Q. Fu, *J. Mater. Chem. C*, 2017, **5**, 3748-3756.
4. B. Zhou, Z. Zhang, Y. Li, G. Han, Y. Feng, B. Wang, D. Zhang, J. Ma and C. Liu, *ACS Appl. Mater. Interfaces*, 2020, **12**, 4895-4905.
5. Z. Ling, C. E. Ren, M. Q. Zhao, J. Yang, J. M. Giammarco, J. Qiu, M. W. Barsoum and Y. Gogotsi, *Proc. Natl. Acad. Sci. U.S.A.*, 2014, **111**, 16676-16681.
6. B. Yuan, C. Bao, X. Qian, L. Song, Q. Tai, K. M. Liew and Y. Hu, *Carbon*, 2014, **75**, 178-189.
7. Q. C. Song, Z. Y. Zhan, B. X. Chen, Z. H. Zhou and C. H. Lu, *Cellulose*, 2020, **27**, 7475-7488.
8. Y.-J. Wan, P.-L. Zhu, S.-H. Yu, R. Sun, C.-P. Wong and W.-H. Liao, *Carbon*, 2017, **122**, 74-81.
9. A. Kumar, R. Anant, K. Kumar, S. S. Chauhan, S. Kumar and R. Kumar, *RSC Adv.*, 2016, **6**, 113405-113414.
10. J. Chen, J. Xu, K. Wang, X. Qian and R. Sun, *ACS Appl. Mater. Interfaces*, 2015, **7**, 15641-15648.